nature portfolio

https://doi.org/10.1038/s41586-025-10077-z

Supplementary information

Fossil isotope evidence for trophic simplification on modern Caribbean reefs

In the format provided by the authors and unedited

Supplementary information

1. Supplementary methods

Organic composition of otoliths. Previous studies have quantified the organic constituents of otoliths[71–75]. In brief, the organic fraction is primarily composed of proteins, especially proteoglycans, collagens, and non-collagen proteins[72,75]. Smaller contributions from polysaccharides such as glycosaminoglycans[76,77] and from lipids[74,78] have also been reported. As the majority of N-containing organic substrates are proteins, we refer to the bulk organic matrix as proteinaceous. In contrast, certain classes of lipids have been identified in coral skeletal matrices, where they are thought to stabilize amorphous calcium carbonate precursors during biomineralization[79,80]. While lipids remain an understudied topic in biomineralization studies[77,79], they typically lack nitrogen and thus here, focusing on otoliths, we describe proteins as the main N-bearing substrate that we oxidize in the laboratory and subsequently measure during carbonate-bound $\delta^{15}N$ analysis. Otolith N content, a proxy for protein content, averaged 36-42 nmol N mg^{-1} across the four fish families analyzed (Gobiidae, Apogonidae, Atherinidae, and Haemulidae), while coral carbonate-bound N content averaged 4.1 ± 0.5 nmol N mg^{-1} (Table S1).

Trophic metrics. The mean trophic level and food chain length were calculated based on measured $\delta^{15}N$ of the fish community (Fig. 3**a**) and on bootstrapped sampling (Fig. 3**d**). We illustrate how these metrics were calculated in *Fig. S1* and in main text Fig. 2c (inset, trophic level calculation) and Fig. 2d (inset, isotopic niche width). We also calculated 'unweighted MTL', the unprocessed mean of all $\delta^{15}N$ measurements from each time period and region (*Table S2, Extended Data Fig. 5*).

Specimen selection. Otoliths were extracted from two coral reef sedimentary deposits that are the only known mid-Holocene otolith-bearing reef sediments in the Caribbean (Fig. 1*, Extended Data Fig.2,* Table S3). Of the otolith specimens that were measured for $\delta^{15}N$, between 30% (grunts) and 100% (silversides) were identified to species-level. When species-level was not feasible due to the challenges in identifying otoliths of juvenile fishes, otoliths were identified to genus- or family-level (Table S4).

Locality information. To sample the geographic and temporal range contained within the fossil and modern reef sediments, otoliths and coral fragments were selected from bulk sediment bags (sample numbers) with unique combinations of locality (site), depth (within each locality), and replicate sample number (two replicates were taken per depth). This sampling approach aimed to reduce potential spatial and temporal biases by sampling each reef deposit broadly. Supplementary Figs. S2 and S3 summarize the distribution of specimens that were analyzed for $\delta^{15}N$ by sub-locality (Fig. S2) and by locality (Fig. S3). Intra- and inter-locality $\delta^{15}N$ variations were similar to one another, showing that $\delta^{15}N$ variation was not driven by the inclusion of sites bearing unique $\delta^{15}N$ patterns.

Otolith-based fish size reconstruction. Fish size reconstructions were based on otolith-fish length relationships derived from locally obtained modern specimens[22]. Otolith length was measured using ImageJ (version: 1.52k). Power law functions for otolith-to-body length conversions were applied for each taxon, revealing fish sizes from 1 to 11 cm (Table S2).

Re-sampling. Bootstrapped community-level trophic metrics were calculated for each region and time period using the measured $\delta^{15}N$ distribution and the taxonomic composition of the fish community (from [22]). Table S5 summarizes the measured $\delta^{15}N$ means, medians, and standard deviations by family for each region and time period, along with imputed bootstrapped means (based on 1,000 draws) and fish community

proportions. These metrics reflect community-wide nitrogen isotope distributions within the time-averaged reef sediments. The high relative abundances of gobies and cardinalfishes reflect their relatively short life spans and high mortality rates, which result in greater accumulation of their otoliths in sediments over time compared to otoliths of longer-lived, lower-turnover taxa. These data were used to calculate $\delta^{15}N$-based trophic structure metrics in the main text (Fig. 2 and Extended Data Figs. 4-6).

2. $\delta^{15}N_{oto}$ comparisons with known dietary patterns

Grunts**,** the most abundant representative of higher trophic level fishes in the fossil sediment record, are omnivorous predators that undergo movements to adjacent habitats, where available, ranging up to 5 km to feed on diverse crustaceans, mollusks, and some fish[81,82]. Prior studies on this group of fishes shows that their $\delta^{15}N$ ranges from 8-10 ‰ in the Caribbean, similar to our results[30,83,84].

Cardinalfishes showed a trophic level (TL) that was similar to that of grunts. Cardinalfishes are distinguished from other cryptobenthic fishes by the relatively higher frequency of teleost prey items in their diet, including fish eggs, larvae, and other parts[29], a factor that generates high trophic positions. There are few isotope studies on this family[30,36,85], but their classification as generalist carnivores is consistent with our relatively high $\delta^{15}N$ observed in our data. One of the most common cardinalfishes[86] in the Caribbean, *Phaeoptyx conklini*, for example, is a nocturnal predator whose prey items include small fish, small crustaceans, polychaete worms, and fish eggs[29].

Silversides, a small schooling fish that feeds on copepods in the water column above coral reefs[51,87,88], occupied an intermediate $\delta^{15}N$ between gobies and the higher trophic level fishes (cardinalfishes and grunts). Their intermediate trophic level was also consistent with stomach content data and previous isotope measurements of fish tissues. Silversides primarily feed on zooplankton such as copepods, although shrimp larvae, fish larvae, polychaete larvae, barnacle larvae, fish scales, and fish eggs have been found in stomachs[51,87,88]. We have found only three studies reporting $\delta^{15}N$ for silversides, which report their $\delta^{15}N$ and trophic position to be slightly higher than that of co-occurring herbivores[31,32,89]. Pelagic $\delta^{15}N$ is higher than benthic $\delta^{15}N$ in many coral reef ecosystems, including in Bocas del Toro, Panama (e.g.,[33,90]). Thus, the intermediate $\delta^{15}N$ of silversides in our study is consistent with their pelagic foraging and their higher $\delta^{15}N$ than gobies, the latter of which are considered primarily benthic foragers (e.g.,[29]).

Gobies showed the lowest relative trophic position, consistent with their known TL patterns based on prey items from stomach content studies[29,91] and stable isotope studies (e.g.,[30]) of modern fishes. Prior isotope studies found these species to be on average 3-4 ‰ lower than co-occurring species of grunts[30], similar to our results.

For a subset of goby otoliths, taxonomic identification allowed for examining genus- or species-level taxonomic patterns in $\delta^{15}N_{oto}$. These taxon-specific $\delta^{15}N$ patterns generally followed the coarser family population-level $\delta^{15}N$ patterns (*Extended Data Fig. 5*). The majority of goby otoliths were from *Coryphopterus personatus* and *C. glaucofraenum*, which are omnivorous cryptobenthic species [92]. *C. personatus* primarily consumes copepods[93,94]. Dietary studies also show relativity high contributions of mangrove-derived nutrients in diets of *C. personatus* during the dry season, perhaps because gobies do not distinguish between mangrove debris and copepods suspended in the water column[93]. *C. glaucofraenum* consumes plants, but also bivalves, ostracods, ophiuroids, and copepods[51]. While still considered benthic, *C. personatus* gobies can switch their foraging behavior to the water column when wave energy and

turbidity are higher[93,95]. In general, $\delta^{15}N_{oto}$ of both *Coryphopterus* species had intermediate $\delta^{15}N_{oto}$ compared to other goby taxa, consistent with their omnivorous and varied diets.

We also measured *Bathygobius* sp., but only in the DR in both time periods, with *Bathygobius* reported to be mainly a generalist detritivore[28]; and *Bollmannia* sp., but only in Panama in both time periods, reported to be a carnivore consuming mobile benthic crustaceans and which tend to be associated with burrows and to live in muddy substrates[88,96,97]. Consistent with these dietary studies, *Bollmannia* had the highest $\delta^{15}N_{oto}$ in both time periods in which it was measured (Panama, both time periods). *Bathygobius* had divergent $\delta^{15}N$ patterns through time, with the lowest $\delta^{15}N_{oto}$ compared to other gobies in the mid-Holocene DR, and among the highest $\delta^{15}N_{oto}$ during the modern DR. Species in the *Elacatinus* genus are the most likely to exhibit cleaning behavior in the Caribbean[98], which could elevate their $\delta^{15}N$ due to feeding on parasites that are feeding on higher trophic level reef fish. However, *Elacatinus* otoliths did not have high $\delta^{15}N$ in our analyzed specimens (*Extended Data Fig. 5)*.

3. Alternative explanations for reduced $\delta^{15}N$ variability

Fish size. Fish size and trophic level (TL) are known to be linked[99]. Thus, the larger isotopic niches observed in our data could be driven by a larger size range of past fishes. We reconstructed fish size (*Supplementary Fig. S4*) based on otolith-fish length relationships from locally obtained modern specimens[22]. Otolith-to-body length conversions were applied for each taxon, revealing fish sizes from 1 to 4.1 cm (cryptobenthic taxa) and up to 11 cm (Haemulidae) (*Extended Data Table 9*). We found that inferred body sizes from otoliths were, overall, unchanged between the two time periods (*Extended Data Fig. 8*) and, for a given size, the $\delta^{15}N_{oto}$ range was narrower today than during the fossil period (*Supplementary Fig. S4*). Thus, the niche width declines were not driven by differences in fish body size.

***Community composition*.** One set of hypotheses for the decreased niche widths of contemporary coral reef fishes involves the potential for shifts in the taxonomic identity of fish in each family, where greater biodiversity could generate greater family-level niche widths in the mid-Holocene. Most significantly, inclusion of otoliths from cleaner fishes in the goby family would have the greatest potential to affect $\delta^{15}N$ at the family level, with fish that eat ectoparasites having potential to be two trophic levels higher than even large reef fishes (e.g., have been shown previously to result in high TL only exceeded by barracuda (*Sphyraena barracuda*); [30]). As noted above (‘*$\delta^{15}N_{oto}$ comparisons with known dietary patterns’*), species in the *Elacatinus* genus are most likely to exhibit cleaning behavior in the Caribbean[98], yet *Elacatinus* $\delta^{15}N_{oto}$ in our data had intermediate $\delta^{15}N$ among our analyzed specimens (*Extended Data Fig. 3)*. Additionally, overall biodiversity curves are similar between the two time periods in each region[22]. While we cannot completely rule out shifts in fish community composition at the species level, most notably among gobies, which are hyper-diverse, the coherent patterns—greater variability, and generally lower mean $\delta^{15}N$ of Holocene gobies in Panama, for example—were observed across all groups even when separating fish by genus or by species, where available, for each family (*Extended Data Fig. 3)*, indicating that larger ecological drivers, not differences in relative abundances of component species, are generating the observed $\delta^{15}N$ patterns.

Time averaging. Another possible explanation is differences in time averaging between mid-Holocene and modern time periods. Greater time averaging could result in including coral and or fish from a greater range of time periods with distinct ecological characteristics or $\delta^{15}N_{base}$ if the mid-Holocene samples encompassed longer durations of time. However, our radiometric dating shows that samples are spanning similar

windows of time, ~100 years, in both time periods (see *Methods*). Coral reef accretion rates have slowed since the mid-Holocene, however, resulting in a pattern in which each mid-Holocene bulk sediment sample tends to encompass a shorter duration of time[4]. Despite the shorter snapshots of Holocene bulk sample bags (the units of sediment sampling), we observe similar variability at the sample bag level (i.e., intra-sample variability; coral in *Fig. S2*) to that observed at the Locality level (i.e., intra-Locality variability, *Fig. S3*) and at the Time Period level (Fig. 3), showing that neither different sites nor differences in time averaging are likely explanations for the declining variability of coral or otolith $\delta^{15}N$. Therefore, the most likely conclusion is that $\delta^{15}N$ patterns were generated by ecological conditions operating on timescales that were captured equally well by our sampling from each time period. While small sample sizes preclude statistical characterization of these patterns, differences in time averaging from different time periods or sample bags do not appear to be driving the $\delta^{15}N$ variability.

Preservation. Preservation could also affect our results, if variations in preservation were greater during one of the time periods and were associated with $\delta^{15}N$ differences. Preservation of organic matter is often examined using N content, the mass-standardized concentration of nitrogen in a sample[100–102]. Diagenetic alteration generates a fingerprint of diagenetic processes, such that highly altered material tends to show an inverse relationship between N content and $\delta^{15}N$ resulting from preferential removal of low $\delta^{15}N$ material in diagenetically altered substrates (e.g., as reviewed in[100]). However, we observed similar patterns in N content, a proxy for preservation of organic matter (e.g., [101]), and no co-variation with $\delta^{15}N$ (Extended Data *Fig. 4*) and similar patterns of N content and N content variability between time periods (*Fig. S5*). Thus, preservation is not a parsimonious explanation either. We interpret patterns in $\delta^{15}N$ as original, as opposed to secondary, isotopic signals preserved in the carbonate biominerals.

4. Ecological explanations for reduced $\delta^{15}N$ variability

Ruling out non-ecological explanations, we turn to known declines in ecosystem health on coral reefs in the Caribbean, to explain the observed niche width and FCL patterns. Previous studies in the region, including at our study sites in Bocas del Toro, Panama and in the DR, have used indicator species to highlight the broader ecological changes occurring in the region (Fig. S6). There are several mechanisms by which ecological changes can explain our observed niche and FCL patterns.

Micro-habitat availability. On small spatial scales, declining micro-habitat availability for small fishes likely contributes to reduced $\delta^{15}N$ variability in modern fish diets, as coral reef microhabitats exhibit distinct prey types and $\delta^{15}N$ signatures at localized scales[36,103]. Mid-Holocene reefs, dominated by *Acropora* spp.[52] likely contained diverse microhabitats and dietary items. *Acropor*a-associated structural complexity is critical for predator refugia and habitat diversity[104,105]. High structural complexity generates a wide range of the shapes and volumes in which fish can find refuge from predation (e.g., [106,107]). The heterogeneity of habitats also increases the habitat volume, surface area, food resources, and number of available niches (e.g., [108,109]). Declines in structural complexity[2] could narrow prey $\delta^{15}N$ diversity, primarily through reduced microhabitat availability and complexity, reducing population niche widths.

Limited access to preferred prey could be driven by declines in specific coral species, which in turn host distinct foraging opportunities. Fast-growing Acroporid corals, *Acropora cervicornis* and *A. palmata*, have declined by 99% in the Caribbean[3,110]. Indeed, fringing reefs in general have become increasingly dominated by more competitive coral taxa, in a shift that has become attributed to land use changes and eutrophication as opposed to disease vulnerability[3]. As fishes can exhibit entirely distinct behavior based

on their coral[104,111,112], changes in coral community writ-large may help to explain the observed fish trophic diversity declines.

Predation pressure (non-consumptive effects of predation). Changes in foraging behavior could also be driven by declines in predation pressure, although cryptobenthic taxa (gobies, cardinalfishes) like those in the our study are relatively invulnerable to top-down control by predators and instead are considered more vulnerable to physical changes in the environment (wave energy, habitat availability) (e.g.,[86]). However, overfishing of top predators and mesopredators may have caused shifts in foraging behavior of cryptobenthic fishes on modern coral reefs. Predation pressure can shape trophic structure, especially when combined with reduced structural complexity of reefs. Specifically, high predation pressure and high habitat complexity causes behavioral patterns in prey fish such that prey fishes experience and forage within only a small subset of the coral reef[113]. Reduced predation pressure can weaken the predator-driven trophic disparity, allowing fish to consume a larger number of prey items and lessening their observed dietary differentiation (e.g.,[44]). Top-down (predator-driven) effects on food web structure are famously challenging to demonstrate in coral reef contexts (e.g.,[114]), but declines in predator abundances are known to have occurred, evidenced by declines in shark dermal denticles[4] and historical losses of large groupers and snappers[115]. These changes could diminish niche widths and trophic diversity of prey fishes, especially when combined with reduced structural complexity and increased foraging range.

Habitat connectivity. Additionally, mid-Holocene fishes may have had greater historical access to foraging in mangroves, which contain relatively high $\delta^{15}N$ prey items[116–118]. Currently, mangroves provide a significant source of food for coral reef animals in the Bocas del Toro food web (e.g., [119]), and mangroves may have had greater contributions in the prehistorical past, prior to coastal development known to have reduced mangroves in the Caribbean[120–123]. This point is supported by the fact that grunts and cardinalfishes—the more mobile groups we examined—exhibited the largest declines in TL over time (Fig. 4a). Grunts forage up to 5 km from their home reefs and cardinalfishes undergo off-reef movements up to 0.5 km[81,82,124]. It has been previously established that variations in habitat use affect observed isotopic niche width, such that more highly migratory or mobile individuals or populations tend to have larger isotopic variations (e.g., [103,125,126]) compared to individuals or populations with high residence time in only one habitat type. Currently, there is no clear evidence that mangrove extent has increased or decreased compared to mid-Holocene, as more stable sea level today would generate more optimal conditions for mangroves compared to the mid-Holocene. At the same time, coastal development is more severe in the neighboring coastlines of south DR compared to the coastline of Panama near our sites and mangroves have declined in both regions over recent decades, leading us to consider that declining mangrove habitat could be an explanation for the more severe $\delta^{15}N$ mean value changes in the DR. Specifically, the widespread decline in mangrove and seagrass extent in the Caribbean—and in study regions specifically has occurred in recent decades[120–123], although longer term data on these habitats is lacking. In food web theory and empirical studies, mobile consumers facilitate longer food chain lengths due to connecting different habitats with distinct energy pathways[127–129]; thus, greater habitat connectivity of prehistorical coral reefs is also consistent with our observation of longer food chains in the past. We conclude that the loss of connectivity with adjacent habitats (e.g., mangroves, seagrasses) may be a major factor leading to the decreased trophic level and the trophic diversity (isotopic niche widths) of taxa with the largest propensity for off-reef movements. Thus, the decline in TL in grunts and cardinalfish may signal a loss of connectivity to adjacent habitats in both regions.

Shifts from benthic to pelagic foraging. Gobies in Panama increased their TL. This increased TL, coupled with the high abundances of gobies, caused the ecosystem MTL to increase slightly (using bootstrapped data; $P<0.001$; *Extended Data Table 2*). The higher TL indicates decreased reliance on benthic-sourced prey and greater consumption of pelagic-sourced organic matter, the latter of which has a higher $\delta^{15}N$ than benthic primary producers[33,90]. Gobies in the *Coryphopterus* genus, which were abundant in our assemblage (*Extended Data Fig. 5*), are known to spend a greater proportion of time feeding in the water column when pelagic food resources increase[93,95]. While still considered benthic, both species shift their foraging behavior to the water column when wave energy, turbidity, or primary productivity are elevated[93,95]. Several lines of evidence (increased terrigenous-sourced organic matter, declining proportions of symbiont-bearing foraminifera, increased N content of seagrasses, and increased chlorophyll concentrations) suggest that Almirante Bay is becoming increasingly eutrophic compared to historical and pre-historical time periods[130–133], a factor that would enhance water column food availability and thus promote pelagic feeding among *Coryphopterus* gobies in response[93,95]. In Bocas del Toro, pelagic primary consumers are ~3‰ higher than benthic primary consumers[33,90]. Additionally, while not widespread from shore, the influence of human-sourced nutrients results in elevated $\delta^{15}N$ of bivalves and gastropods closest to shore[134]. The higher modern $\delta^{15}N$ across each level of taxonomic resolution for gobies (Extended Data Fig. 5) is consistent with their greater reliance on pelagic prey (e.g., copepods) rather than benthic crustaceans or detrital material.

Gobies increased $\delta^{15}N$ in Panama, consistent with a shift from benthic (lower $\delta^{15}N$) to pelagic (higher $\delta^{15}N$) foraging, perhaps in response to greater food availability in the latter. Gobies range from dietary specialists to generalists, with diets composed of coral tissue and mucous[135] to fish eggs, copepods, mollusks, small invertebrates, detritus, algae, and parasites (i.e., cleaner fishes)[29,91]. Some are herbivores consuming filamentous algae[91]. The majority of goby otoliths were from *Coryphopterus personatus* and *C. glaucofraenum*, two species of omnivorous cryptobenthic species that primarily consume copepods but also bivalves, ostracods, and small echinoderms[92].

Shifts in the community composition of pelagic ichthyoplankton. Declines in abundances of high trophic level fishes[115,136,137] also means declines in the eggs of these higher trophic level fishes, which is one way in which non-targeted, low TL fishes could have their food availability—and therefore their $\delta^{15}N$—be indirectly affected by fishing. Widespread declines in parrotfishes (e.g., [138,139]), a low TL taxon, could also mean decreases in the proportion of the lowest TL ichthyoplankton. However, we rule out ichthyoplankton changes as a primary driver as the largest changes in both niche width and TL were observed in grunts and cardinalfishes, both of which are known to undergo relatively large off-reef foraging forays (while reef fish ichthyoplankton abundances are centered on-reef) and consume large proportions of benthic crustaceans as opposed to ichthyoplankton.

5. Panama *vs*. DR coastal health comparisons

In an assessment of global coastal regions with the greatest vulnerability and greatest potential gains from conservation, the DR was among the most likely regions to gain from mangrove and coral reef protection[140] due to hurricane vulnerability, forecasted sea level changes, likelihood of bleaching, and mangrove areas lost to-date. Today, the DR has less mangrove extent relative to Bocas del Toro Panama, and has experienced a greater degree of mangrove and seagrass loss[141,142]. Along the southern coast of the DR, the spatial extent of mangroves was 42 km² in 2020, approximately 12% of the 828 km of the coastline, compared to in the Bocas del Toro archipelago alone (including the area of Laguna de Chiriquí),

approximately 40% of the coastline is mangrove (18 km^2 of the 894 km of coastline estimated linearly)[123,143].

Studies in Bocas del Toro show that mangrove-sourced food remains important to modern fishes. In a study focused on sessile invertebrates on coral reefs in Bocas del Toro, including sponges, file clams, and feather duster worms, mangrove-sourced contributions were frequently a large percentage of dissolved organic matter (DOM) filtered by these organisms, ranging from 0 to 60% of DOM sources[144]. In another study focused on reef fish communities in Bocas del Toro, proximity to mangrove habitat was a correlate of reef fish abundance and biodiversity[119].

Analogous studies of mangrove-derived subsidies do not exist for the DR. Yet studies show that coral reefs in general are in decline in the DR. All predatory fishes have low abundances; predatory fishes in the serranid family, for example, declined most steeply by 80%[142] since monitoring began in 2015. Additionally, all coral reefs in DR are considered threatened[8]. DR country-wide status is that coral cover has been declining on average 5% per year since 2015[142].

6. Niche width and ecosystem stability

The implications of dietary diversity for food web stability continue to be debated[128,145,146], with variability in diet and dietary resources serving as a buffer or as a vulnerability in different contexts depending on the interaction strengths of specific trophic linkages[42,129,147–151] and the timescales over which trophic linkages occur or are observed[128,152–154]. However, intra-population variability in (realized/ phenotypic) niche (i.e., the 'portfolio effect') has generally been considered to be a successful bet-hedging strategy against changes in prey availability or environmental conditions[127,155]. The portfolio effect increases stability by increasing the compartmentalization or modularity of food web structure[42]. Intra-population (intra-specific) specialization can be considered a form of compartmentalization by (1) increasing the interaction strength between a given pairing of prey and consumer and by (2) simultaneously decreasing the interaction strength between that pairing (i.e., that subset of the food web) and the rest of the food web[40,145,156]. Inter-individual niche differentiation (specialization) therefore increase food web stability[40,156], as perturbations become constrained to a subset of consumers. Food webs containing multiple channels of energy are considered more stable[42,127,157].

Some species respond to environmental perturbations by changing their diet[18,49,158]. Behavioral flexibility is one way in which fish species mitigate environmental changes (although these changes may occur at a physiological cost[159]). Multiple studies show that predators with flexible foraging strategies are resilient to the effects of habitat degradation (e.g.,[12,32,49,158]) and this behavioral flexibility has been explored as a mechanisms providing stability to food web structure[152]. Consequently, the increased trophic similarity may indicate increased trophic redundancy (e.g., [7]), often considered a factor that leads to increased stability to perturbations (e.g., in food supply). This last observation leads to the hypothesis that the current configuration—i.e., narrower population-level isotopic niche widths—may represent a more stable food web network, albeit one in which increased competition for resources may lead to other dynamics[160,161].

However, ecological theory and observations point to our preferred hypothesis—i.e., that increased trophic similarity among individual fish indicates decreased stability, as all individuals in a given family now rely on a common pool of overlapping resources—as being more likely. Behavioral flexibility only generates trophic redundancy to a point—once the pool of resources is so evenly shared that trophic redundancy leads

to competition, a destabilizing force, then collapsed niche widths can potentially lead to extinction or other forms of decreased persistence within the food web[145,160,162–164].

References

71. Thomas, O. R. *et al.* The inner ear proteome of fish. *FEBS J.* **286**, 66–81 (2018).
72. Thomas, O. R. B. & Swearer, S. E. Otolith Biochemistry — A Review. *Rev. Fish. Sci. Aquac.* **27**, 458–489 (2019).
73. Borelli, G., Mayer-Gostan, N., De Pontual, H., Boeuf, G. & Payan, P. Biochemical relationships between endolymph and otolith matrix in the trout (*Oncorhynchus mykiss*) and turbot (*Psetta maxima*). *Calcif. Tissue Int.* **69**, 356–364 (2001).
74. Payan, P., De Pontual, H., Bœuf, G. & Mayer-Gostan, N. Endolymph chemistry and otolith growth in fish. *Comptes Rendus - Palevol* **3**, 535–547 (2004).
75. Hüssy, K. *et al.* Trace Element Patterns in Otoliths: The Role of Biomineralization. *Rev. Fish. Sci. Aquac.* **29**, 445–477 (2021).
76. Dauphin, Y. & Dufour, E. Composition and properties of the soluble organic matrix of the otolith of a marine fish: *Gadus morhua* Linne, 1758 (Teleostei, Gadidae). *Comp. Biochem. Physiol. Part A Mol. Integr. Physiol.* **134**, 551–561 (2003).
77. Takagi, Y., Ishida, K. & Mugiya, Y. Carbohydrates of the otolith organ in the rainbow trout *Oncorhynchus mykiss* detected by lectins. *Fish. Sci.* **66**, 933–939 (2000).
78. Gillikin, D. P. *et al.* High-resolution nitrogen stable isotope sclerochronology of bivalve shell carbonate-bound organics. *Geochim. Cosmochim. Acta* **200**, 55–66 (2017).
79. Reggi, M. *et al.* Influence of intra-skeletal coral lipids on calcium carbonate precipitation. *CrystEngComm* **18**, 8829–8833 (2016).
80. Falini, G., Fermani, S. & Goffredo, S. Coral biomineralization: A focus on intra-skeletal organic matrix and calcification. *Semin. Cell Dev. Biol.* **46**, 17–26 (2015).
81. Verweij, M. C., Nagelkerken, I., Wartenbergh, S. L. J., Pen, I. R. & Van Der Velde, G. Caribbean mangroves and seagrass beds as daytime feeding habitats for juvenile French grunts, Haemulon flavolineatum. *Mar. Biol.* **149**, 1291–1299 (2006).
82. Nagelkerken, I., Bothwell, J., Nemeth, R. S., Pitt, J. M. & Van Der Velde, G. Interlinkage between Caribbean coral reefs and seagrass beds through feeding migrations by grunts (Haemulidae) depends on habitat accessibility. *Mar. Ecol. Prog. Ser.* **368**, 155–164 (2008).
83. Stuthmann, L. E., Castellanos-Galindo, G. A. & Robertson, D. R. The functional ecology of mangrove fishes across the Isthmus of Panama. *Divers. Distrib.* **28**, 1663–1679 (2022).
84. Keegan, W. F. & DeNiro, M. J. Stable Carbon- and Nitrogen-Isotope Ratios of Bone Collagen Used to Study Coral-Reef and Terrestrial Components of Prehistoric Bahamian Diet. *Am. Antiq.* **53**, 320–336 (1988).
85. Wyatt, A. S. J., Waite, A. M. & Humphries, S. Stable isotope analysis reveals community-level variation in fish trophodynamics across a fringing coral reef. *Coral Reefs* **31**, 1029–1044 (2012).
86. Harborne, A. R., Jelks, H. L., Smith-Vaniz, W. F. & Rocha, L. A. Abiotic and biotic controls of cryptobenthic fish assemblages across a Caribbean seascape. *Coral Reefs* **31**, 977–990 (2012).
87. Holzman, R., Ohavia, M., Vaknin, R. & Genin, A. Abundance and distribution of nocturnal fishes over a coral reef during the night. *Mar. Ecol. Prog. Ser.* **342**, 205–215 (2007).
88. Robertson, D. R. & Tassell, J. Van. Bollmannia. *Shorefishes of the Greater Caribbean: online information system* (2019).
89. Yin, H. *et al.* δ13C and δ15N stable isotopes demonstrate seasonal changes in the food web of coral reefs at the Wuzhizhou Island of the South China sea. *Ecol. Indic.* **146**, 109852 (2023).
90. Barragán-Barrera, D. C. *et al.* Foraging habits and levels of mercury in a resident population of bottlenose dolphins (*Tursiops truncatus*) in Bocas del Toro Archipelago, Caribbean Sea, Panama. *Mar. Pollut. Bull.* **145**, 343–356 (2019).
91. Depczynski, M. & Bellwood, D. R. Microhabitat utilisation patterns in cryptobenthic coral reef fish communities. *Mar. Biol.* **145**, 455–463 (2004).
92. Opitz, S. *Trophic interactions in Caribbean coral reefs*. (International Center for Living Aquatic Resources, 1996).
93. Carreón-Palau, L., Parrish, C. C., del Angel-Rodríguez, J. A., Pérez-España, H. & Aguiñiga-García, S. Revealing organic carbon sources fueling a coral reef food web in the Gulf of Mexico using stable isotopes and fatty acids. *Limnol. Oceanogr.* **58**, 593–612 (2013).
94. Santander-Monsalvo, J. Ecología trófica de los peces más abundantes del Parque Nacional Sistema Arrecifal Veracruzano. (Universidad Veracruzana, 2010).
95. Kramer, A., Van Tassell, J. L. & Patzner, R. A. Dentition, diet and behaviour of six gobiid species (Gobiidae) in the Caribbean Sea. *Cybium* **33**, 107–121 (2009).

96. Kramer, A., Kovačić, M. & Patzner, R. A. Dentition of eight species of Mediterranean Sea Gobiidae: Do dentition characters of gobies reflect phylogenetic relationships? *J. Fish Biol.* **80**, 29–48 (2012).
97. Tornabene, L., Van Tassell, J. L., Robertson, D. R. & Baldwin, C. C. Repeated invasions into the twilight zone: evolutionary origins of a novel assemblage of fishes from deep Caribbean reefs. *Mol. Ecol.* **25**, 3662–3682 (2016).
98. Huie, J. M., Thacker, C. E. & Tornabene, L. Co-evolution of cleaning and feeding morphology in western Atlantic and eastern Pacific gobies. *Evolution (N. Y).* **74**, 419–433 (2020).
99. Dunic, J. C. & Baum, J. K. Size structuring and allometric scaling relationships in coral reef fishes. *J. Anim. Ecol.* **86**, 577–589 (2017).
100. Robinson, R. S. *et al.* A review of nitrogen isotopic alteration in marine sediments. *Paleoceanography* **27**, (2012).
101. Ingalls, A. E., Lee, C. & Druffel, E. R. M. Preservation of organic matter in mound-forming coral skeletons. *Geochim. Cosmochim. Acta* **67**, 2827–2841 (2003).
102. Silfer, J. A., Engel, M. H. & Macko, S. A. Kinetic fractionation of stable carbon and nitrogen isotopes during peptide-bond hydrolysis - experimental-evidence and geochemical implications. *Chem. Geol.* **101**, 211–221 (1992).
103. Zapata-Hernández, G. *et al.* Tracing trophic pathways through the marine ecosystem of Rapa Nui (Easter Island). *Aquat. Conserv. Mar. Freshw. Ecosyst.* **31**, 304–323 (2021).
104. Agudo-Adriani, E. A., Cappelletto, J., Cavada-Blanco, F. & Croquer, A. Colony geometry and structural complexity of the endangered species Acropora cervicornis partly explains the structure of their associated fish assemblage. *PeerJ* **2016**, (2016).
105. Wilson, S. K. *et al.* Exploitation and habitat degradation as agents of change within coral reef fish communities. *Glob. Chang. Biol.* **14**, 2796–2809 (2008).
106. Friedlander, A. M. & Parrish, J. D. Habitat characteristics affecting fish assemblages on a Hawaiian coral reef. *J. Exp. Mar. Bio. Ecol.* **224**, 1–30 (1998).
107. Rogers, A., Blanchard, J. L. & Mumby, P. J. Vulnerability of coral reef fisheries to a loss of structural complexity. *Curr. Biol.* **24**, 1000–1005 (2014).
108. Magel, J. M. T., Burns, J. H. R., Gates, R. D. & Baum, J. K. Effects of bleaching-associated mass coral mortality on reef structural complexity across a gradient of local disturbance. *Sci. Rep.* **9**, 1–12 (2019).
109. Roff, G., Joseph, J. & J. Mumby, P. Multi-decadal changes in structural complexity following mass coral mortality on a Caribbean reef. *Biogeosciences* **17**, 5909–5918 (2020).
110. Jackson, J. B. C., Donovan, M. K., Cramer, K. & Lam, V. *Status and Trends of Caribbean Coral Reefs*. *Global Coral Reef Monitoring Network, IUCN* (2014).
111. Whiteman, E. A. & Côté, I. M. Cleaning activity of two Caribbean cleaning gobies: Intra- and interspecific comparisons. *J. Fish Biol.* **60**, 1443–1458 (2002).
112. Taylor, M. S. & Van Tassell, J. L. Observations on microhabitat utilization by three widely distributed neotropical gobies of the genus *Elacatinus*. *Copeia* **2002**, 1134–1136 (2002).
113. McCormick, M. I., Fakan, E. P. & Palacios, M. M. Habitat degradation and predators have independent trait-mediated effects on prey. *Sci. Rep.* **9**, 1–11 (2019).
114. Casey, J. M. *et al.* A test of trophic cascade theory: fish and benthic assemblages across a predator density gradient on coral reefs. *Oecologia* **183**, 161–175 (2017).
115. Wing, S. R. & Wing, E. Prehistoric fisheries in the Caribbean. *Coral Reefs* **20**, 1–8 (2001).
116. Nagelkerken, I. & Van Der Velde, G. Are Caribbean mangroves important feeding grounds for juvenile reef fish from adjacent seagrass beds? *Mar. Ecol. Prog. Ser.* **274**, 143–151 (2004).
117. Briand, M. J., Bonnet, X., Guillou, G. & Letourneur, Y. Complex food webs in highly diversified coral reefs: Insights from $\delta^{13}C$ and $\delta^{15}N$ stable isotopes. *Food Webs* **8**, 12–22 (2016).
118. Kolasinski, J. *et al.* Stable isotopes reveal spatial variability in the trophic structure of a macro-benthic invertebrate community in a tropical coral reef. *Rapid Commun. Mass Spectrom.* **30**, 433–446 (2016).
119. Seemann, J., Yingst, A., Stuart-Smith, R. D., Edgar, G. J. & Altieri, A. H. The importance of sponges and mangroves in supporting fish communities on degraded coral reefs in Caribbean Panama. *PeerJ* **2018**, 1–22 (2018).
120. Recio, M. E., Kuper, J., Vallejo, M., Sommerville, M. & Nayna, J. *Central America mangroves, tenure, and Redd+ assessment*. *USAID Tenure and Global Climate Change Program.* (2016).
121. Van Tussenbroek, B. I. *et al.* Caribbean-wide, long-term study of seagrass beds reveals local variations, shifts in community structure and occasional collapse. *PLoS One* **9**, (2014).
122. ANAM-ARAP (Autoridad Nacional del Ambiente y Autoridad de los Recursos Acu´aticos de Panama). *Manglares de Panamá: importancia, mejores prácticas y regulaciones vigentes*. (2013).
123. Bunting, P. *et al.* Global Mangrove Extent Change 1996 – 2020: Global Mangrove. *Remote Sens.* **14**, 1–32

(2022).
124. Collins, W. P., Bellwood, D. R. & Morais, R. A. Small coral reef fishes with large ecological footprints. *Coral Reefs* (2023). doi:10.1007/s00338-023-02384-6
125. Reddin, C. J., Bothwell, J. H., O'Connor, N. E. & Harrod, C. The effects of spatial scale and isoscape on consumer isotopic niche width. *Funct. Ecol.* **32**, 904–915 (2018).
126. Daban, P., Hillinger, A., Mucientes, G., Blanco, A. & Alonso-Fernández, A. Movement ecology determines isotopic niche width in the undulate skate Raja undulata. *Mar. Ecol. Prog. Ser.* **731**, 147–158 (2024).
127. Rooney, N., McCann, K., Gellner, G. & Moore, J. C. Structural asymmetry and the stability of diverse food webs. *Nature* **442**, 265–269 (2006).
128. Rooney, N. & McCann, K. S. Integrating food web diversity, structure and stability. *Trends Ecol. Evol.* **27**, 40–46 (2012).
129. McCann, K. S., Rasmussen, J. B. & Umbanhowar, J. The dynamics of spatially coupled food webs. *Ecol. Lett.* **8**, 513–523 (2005).
130. Gaubert-Boussarie, J., Altieri, A. H., Emmett Duffy, J. & Campbell, J. E. Seagrass structural and elemental indicators reveal high nutrient availability within a tropical lagoon in Panama. *PeerJ* **9**, 1–21 (2021).
131. Aronson, R. B., Hilbun, N. L., Bianchi, T. S., Filley, T. R. & McKee, B. A. Land use, water quality, and the history of coral assemblages at Bocas del Toro, Panamá. *Mar. Ecol. Prog. Ser.* **504**, 159–170 (2014).
132. Cramer, K. L., O'Dea, A., Leonard-Pingel, J. S. & Norris, R. D. Millennial-scale change in the structure of a Caribbean reef ecosystem and the role of human and natural disturbance. *Ecography.* **43**, 283–293 (2019).
133. Seemann, J. *et al.* Assessing the ecological effects of human impacts on coral reefs in Bocas del Toro, Panama. *Environ. Monit. Assess.* **186**, 1747–1763 (2014).
134. Graniero, L. E., Grossman, E. L. & O'Dea, A. Stable isotopes in bivalves as indicators of nutrient source in coastal waters in the Bocas del Toro Archipelago, Panama. *PeerJ* **2016**, 1–20 (2016).
135. Cole, A. J., Pratchett, M. S. & Jones, G. P. Diversity and functional importance of coral-feeding fishes on tropical coral reefs. *Fish Fish.* **9**, 286–307 (2008).
136. Wake, T. A., Doughty, D. R. & Kay, M. Archaeological investigations provide Late Holocene baseline ecological data for Bocas del Toro, Panama. *Bull. Mar. Sci.* **89**, 1015–1035 (2013).
137. Wing, E. S. The sustainability of resources used by native Americans on four Caribbean Islands. *Int. J. Osteoarchaeol.* **11**, 112–126 (2001).
138. Muraoka, W. T. *et al.* Historical declines in parrotfish on Belizean coral reefs linked to shifts in reef exploitation following European colonization. *Front. Ecol. Evol.* **10**, 1–17 (2022).
139. Mumby, P. J. *et al.* Fishing down a Caribbean food web relaxes trophic cascades. *Mar. Ecol. Prog. Ser.* **445**, 13–24 (2012).
140. Jones, H. P. *et al.* Global hotspots for coastal ecosystem-based adaptation. *PLoS One* **15**, 1–17 (2020).
141. Steneck, R. S. & Torres, R. E. *Estado y tendencias de los arrecifes coralinos en la República Dominicana 2015-2019. Status and trends of coral reefs in the Dominican Republic 2015-2019*. (2019).
142. Steneck, R. S. & Torres, R. Trends in Dominican Republic Coral Reef Biodiversity 2015–2022. *Diversity* **15**, 389 (2023).
143. Bunting, P. *et al.* The global mangrove watch - A new 2010 global baseline of mangrove extent. *Remote Sens.* **10**, (2018).
144. Granek, E. F., Compton, J. E. & Phillips, D. L. Mangrove-exported nutrient incorporation by sessile coral reef invertebrates. *Ecosystems* **12**, 462–472 (2009).
145. Noto, A. E. & Gouhier, T. C. The effects of intraspecific and interspecific diversity on food web stability. *Theor. Ecol.* **13**, 399–407 (2020).
146. Beckerman, A. P., Petchey, O. L. & Warren, P. H. Foraging biology predicts food web complexity. *Proc. Natl. Acad. Sci. U. S. A.* **103**, 13745–13749 (2006).
147. McCann, K. S. The diversity–stability debate. *Nature* **405**, 228–233 (2000).
148. Wootton, K. L. Omnivory and stability in freshwater habitats: Does theory match reality? *Freshw. Biol.* **62**, 821–832 (2017).
149. Kratina, P., LeCraw, R. M., Ingram, T. & Anholt, B. R. Stability and persistence of food webs with omnivory: Is there a general pattern? *Ecosphere* **3**, art50 (2012).
150. Emmerson, M. & Yearsley, J. M. Weak interactions, omnivory and emergent food-web properties. *Proc. R. Soc. B Biol. Sci.* **271**, 397–405 (2004).
151. Gilarranz, L. J., Mora, C. & Bascompte, J. Anthropogenic effects are associated with a lower persistence of marine food webs. *Nat. Commun.* **7**, (2016).
152. Kondoh, M. Foraging Adaptation and the. *Science.* **299**, 1388–1391 (2003).
153. McMeans, B. C. *et al.* Consumer trophic positions respond variably to seasonally fluctuating environments. *Ecology* **100**, 1–10 (2019).

154. Ushio, M. *et al.* Fluctuating interaction network and time-varying stability of a natural fish community. *Nature* **554**, 360–363 (2018).
155. McCann, K. & Hastings, A. Re-evaluating the omnivory-stability relationship in food webs. *Proc. R. Soc. B Biol. Sci.* **264**, 1249–1254 (1997).
156. Elliott Smith, E. A., Harrod, C., Docmac, F. & Newsome, S. D. Intraspecific variation and energy channel coupling within a Chilean kelp forest. *Ecology* **102**, 1–13 (2021).
157. Keppeler, F. W. *et al.* Body size, trophic position, and the coupling of different energy pathways across a saltmarsh landscape. *Limnol. Oceanogr. Lett.* **6**, 360–368 (2021).
158. Karkarey, R., Alcoverro, T., Kumar, S. & Arthur, R. Coping with catastrophe: foraging plasticity enables a benthic predator to survive in rapidly degrading coral reefs. *Anim. Behav.* **131**, 13–22 (2017).
159. Caley, M. J. & Munday, P. L. Growth trades off with habitat specialization. *Proc. R. Soc. B Biol. Sci.* **270**, 175–177 (2003).
160. Bastolla, U. *et al.* The architecture of mutualistic networks minimizes competition and increases biodiversity. *Nature* **458**, 1018–1020 (2009).
161. Cosmo, L. G. *et al.* Indirect effects shape species fitness in coevolved mutualistic networks. *Nature* **619**, 788–792 (2023).
162. Bolnick, D. I. *et al.* The ecology of individuals: Incidence and implications of individual specialization. *Am. Nat.* **161**, 1–28 (2003).
163. Araújo, M. S. *et al.* Network analysis reveals contrasting effects of intraspecific competition on individual vs. population diets. *Ecology* **89**, 1981–1993 (2008).
164. Bolnick, D. I. *et al.* Ecological release from interspecific competition leads to decoupled changes in population and individual niche width. *Proc. R. Soc. B Biol. Sci.* **277**, 1789–1797 (2010).
165. O'Dea, A. *et al.* Prehistoric archives reveal evidence of predator loss and prey release in Caribbean reef fish communities. *Proc. Natl. Acad. Sci. U. S. A.* **122**, (2025).
166. Figuerola, B., Grossman, E. L., Lucey, N., Leonard, N. D. & O'Dea, A. Millennial-scale change on a Caribbean reef system that experiences hypoxia. *Ecography.* **44**, 1270–1282 (2021).
167. Hynes, M. G., O'Dea, A., Webster, J. M. & Renema, W. RADReef: A global Holocene Reef Rate of Accretion Dataset. *Sci. Data* **11**, 1–11 (2024).

Supplementary figures and tables

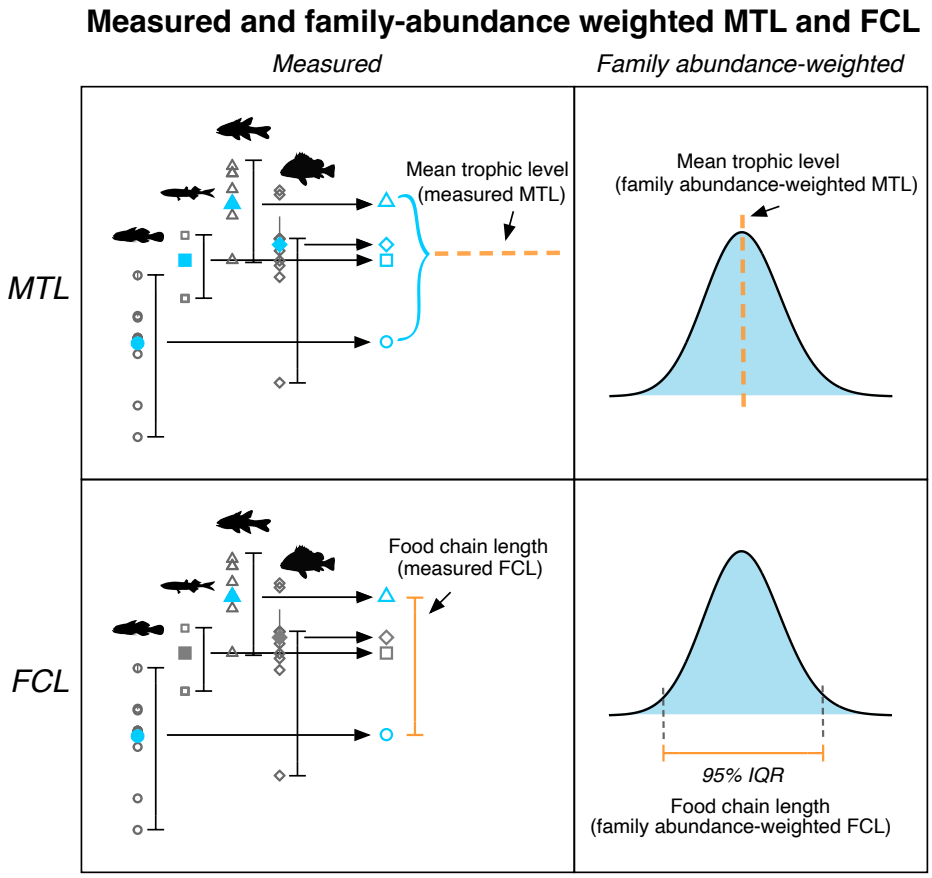

Fig. S1 | Illustrations of measured (left) and bootstrapped family-abundance weighted (right) mean trophic level (MTL) and food chain length (FCL). Measured MTL and FCL estimates are based on the taxon-specific means of measured $\delta^{15}N$; family abundance-weighted metrics are based on the $\delta^{15}N$ distribution obtained from bootstrapping. See also main text Fig. 2c and d for illustrations of how $\delta^{15}N$ measurements are used to calculate taxon-specific trophic level and isotopic niche width.

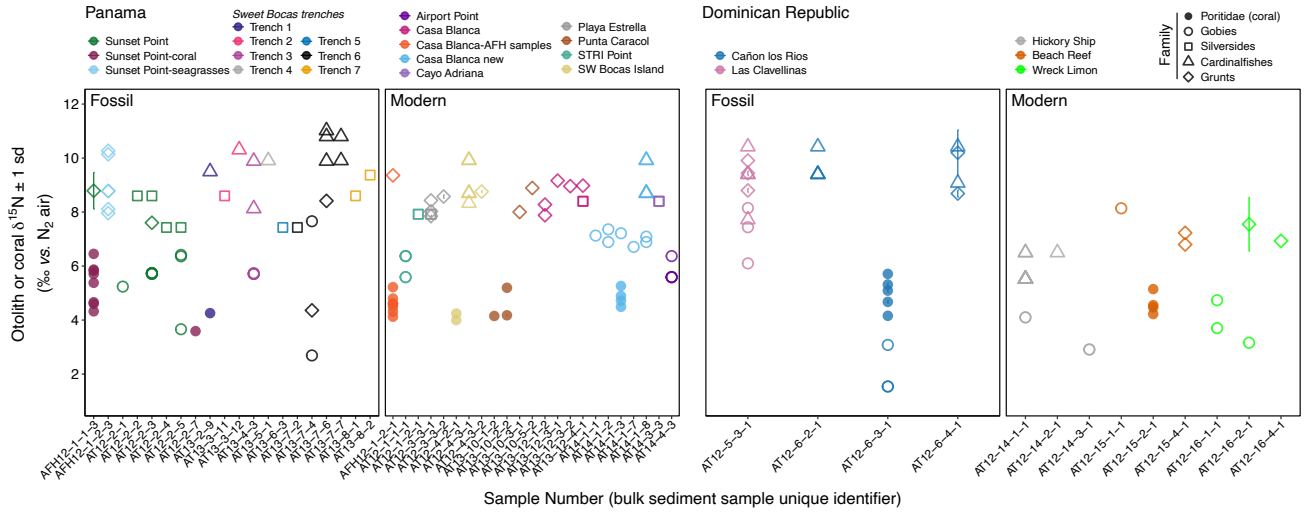

Fig. S2 | All measurements plotted by sub-Locality (sub-site). Each sample number (x-axis) specifies a unique combination of depth, locality, and replicate sediment bag. Co-occurring specimens of corals, gobies, silversides, grunts, and cardinalfishes were measured where possible. Where error bars are shown, they denote the 1 sd of technical replicates—specifically, for some Haemulidae otoliths, which were relatively large, and for each coral fragment. For large Haemulidae otoliths, each otolith was pulverized into a fine powder, the powder was subsampled, and the two subsamples were run separately as technical replicates (see *Methods*). The symbol and error bars for these Haemulidae otoliths are shown as the mean ± 1 sd of the replicate measurements. Additionally, each coral mean $\delta^{15}N$ is comprised of two technical replicates that were averaged to generate a specimen (coral fragment) specific mean $\delta^{15}N$.

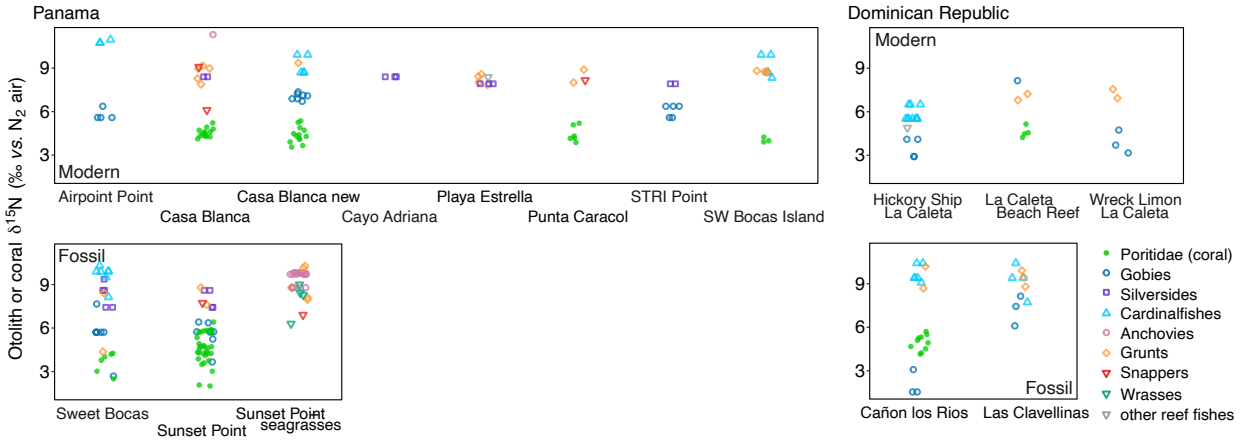

Fig. S3 | All taxa plotted by Locality. Horizontal scatter ("jitter") was added randomly in R to all datapoints to reduce overplotting. Color and symbol correspond to taxa. There are no clear Locality-level patterns in $\delta^{15}N$ within or across taxa, other than gobies in the two mid-Holocene DR sites (goby $\delta^{15}N_{oto}$ was higher in Las Clavellinas and lower in Cañon los Rios). Otoliths sampled from Sunset Point seagrasses and Sunset Point Coral show similar patterns for the grunts, the only species found in both localities. Measurements of otoliths from other reef fishes were measured but not included in the analysis reported in the main text due to a lack of conspecifics for comparison. These otoliths were from fish in the following families: Engraulidae (anchovies, pink open round symbols; *n*=21), Lutjanidae (snappers, red triangle symbols; *n*=8), Serranidae (wrasses; *n*=4), and Gerreidae ('other reef fishes' above; *n*=2). Where error bars are shown, they denote the 1 sd of technical replicates as in Fig. S2.

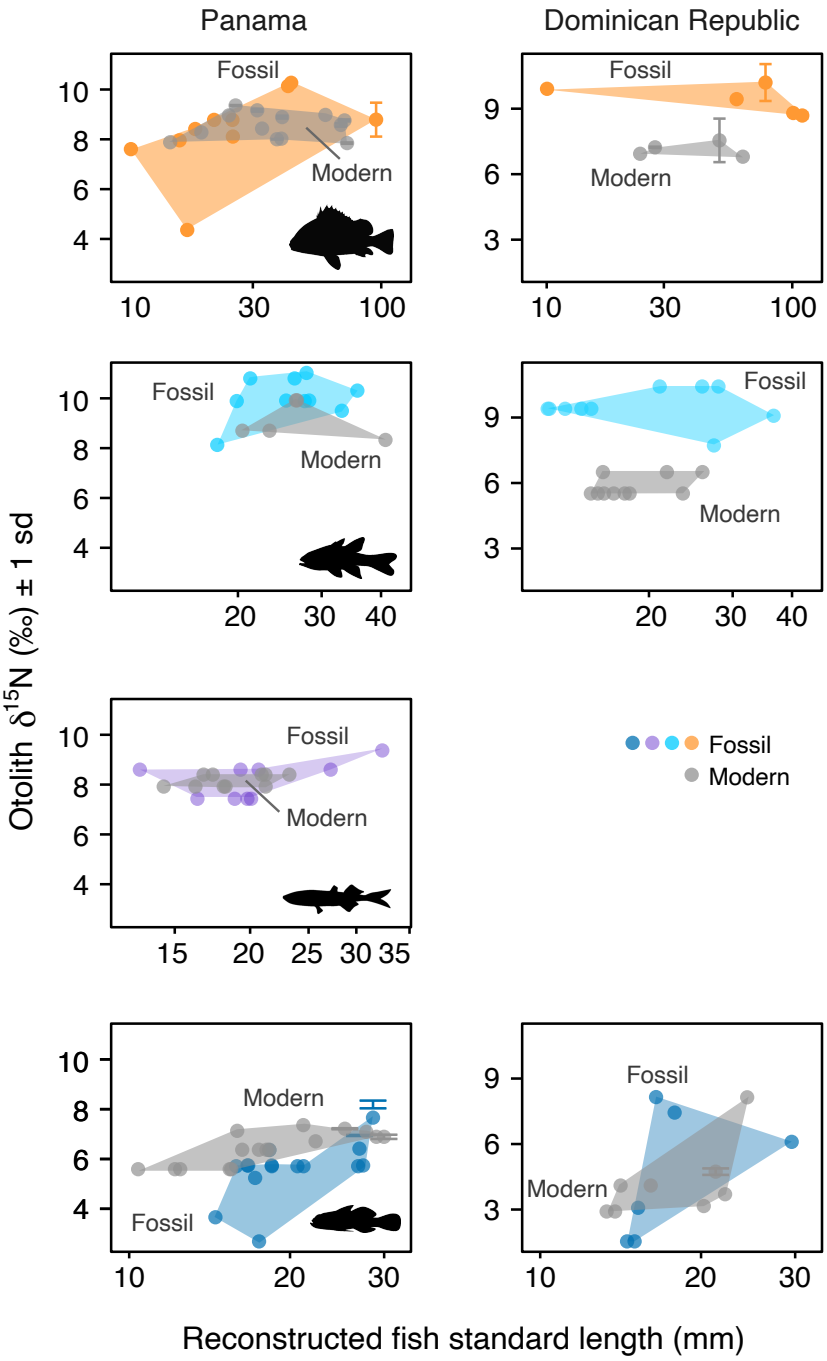

Fig. S4 | Taxon-specific trophic level patterns *vs.* reconstructed fish size (mm). Each symbol represents an individual fish except for several measurements for which multiple otoliths were combined in an initial batch of measurements (see *Extended Data Fig. 4*). See also *Extended Data Fig. 8* for community overview of fish size and $\delta^{15}N$.

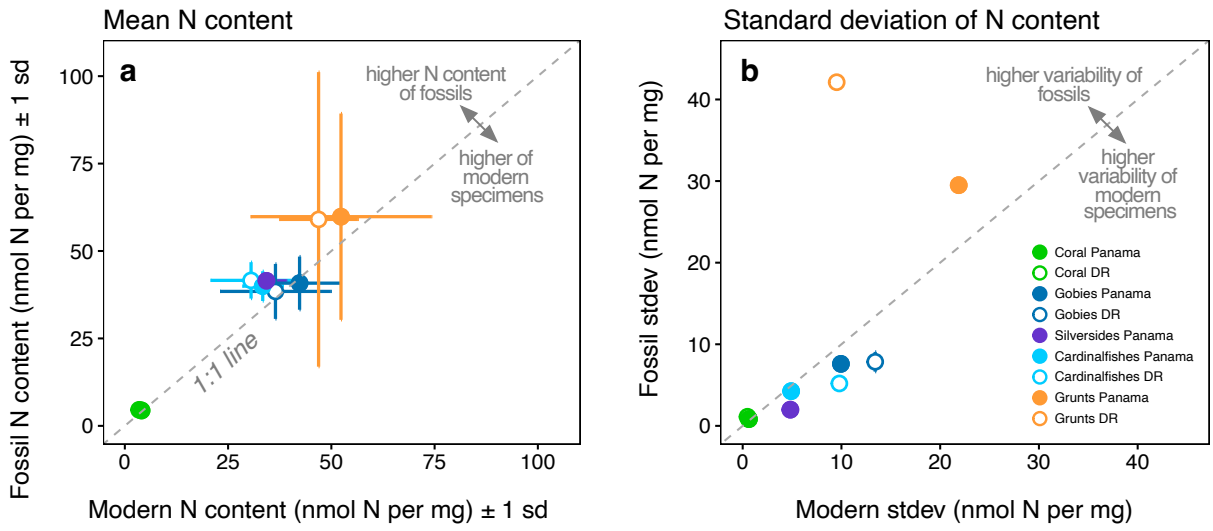

Fig. S5 | Mean N content and N content variation (1 SD). a, Mean N content of fossil *vs*. modern otoliths and corals from the same groups. Each symbol represents the family-specific mean ± 1 sd of N content (nmol N per mg carbonate), a proxy for protein content (see Supplementary information section titled, '*Organic composition of otoliths*'). Filled symbols represent data from Panama and open symbols represent data from the Dominican Republic. **b,** Variation (1 sd) of N content of fossil *vs.* modern otoliths and corals from the same groups. Each symbol represents the family-specific standard deviation of N content. The narrower niche widths (lower $\delta^{15}N$ variability) observed among modern otoliths (Fig. 2d) were not accompanied by similar patterns in N content, a proxy for organic matter content, showing that the higher N isotopic variability of historical samples is not driven by a lower degree of preservation.

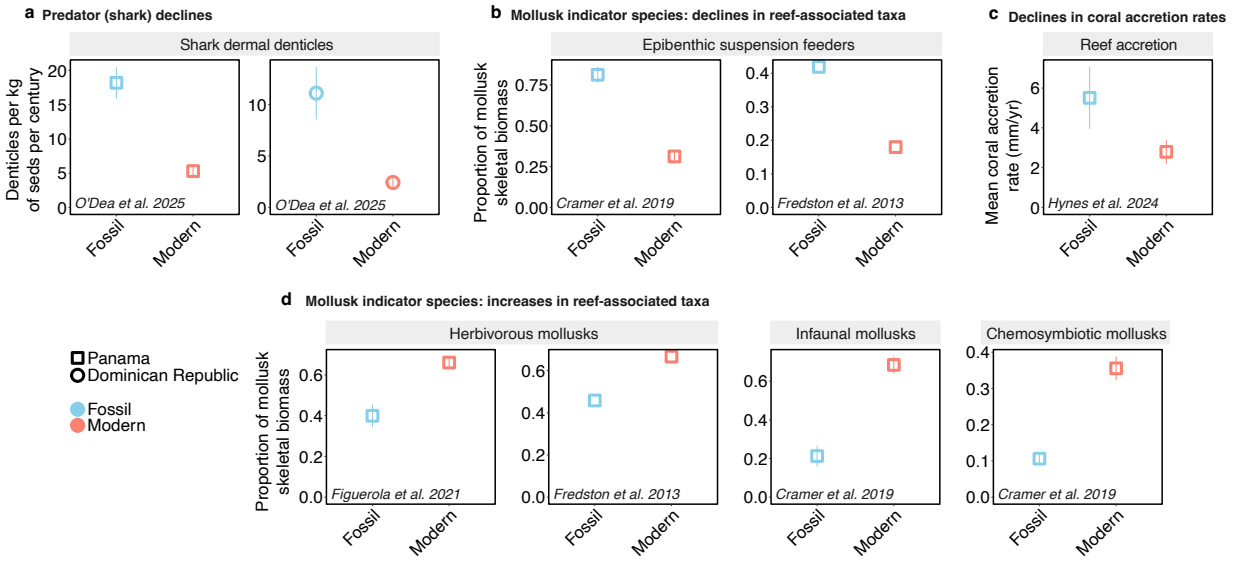

Fig. S6 | Supporting data from previously published studies. Supporting data showing fossil *vs*. modern comparisons of proxies of shark abundances[165], mollusk community composition[56,132,166], and coral reef accretion rates[167] from the same sample sites as the otoliths and corals in our study. **a**, The accumulation rates[165] of shark dermal denticles has declined on reefs in the DR and in Panama. **b**, The relative proportion of suspension-feeding mollusks, which serves as an indicator of water quality (with suspension feeders having higher proportions in oligotrophic environments[56,132,166]), have declined relative to the rest of the mollusk community. **c**, The coral reef accretion rate has declined[167], showing that the health of the reef has been negatively impacted since the mid-Holocene. **d**, Mollusks groups showing increased relative abundance in response to water quality and ecosystem health changes, including benthic herbivorous mollusks, infaunal mollusks, and infaunal deposit-feeding chemosymbiotic bivalves, consistent with increased turf algae and decreased water quality on modern reefs[56,132,166].

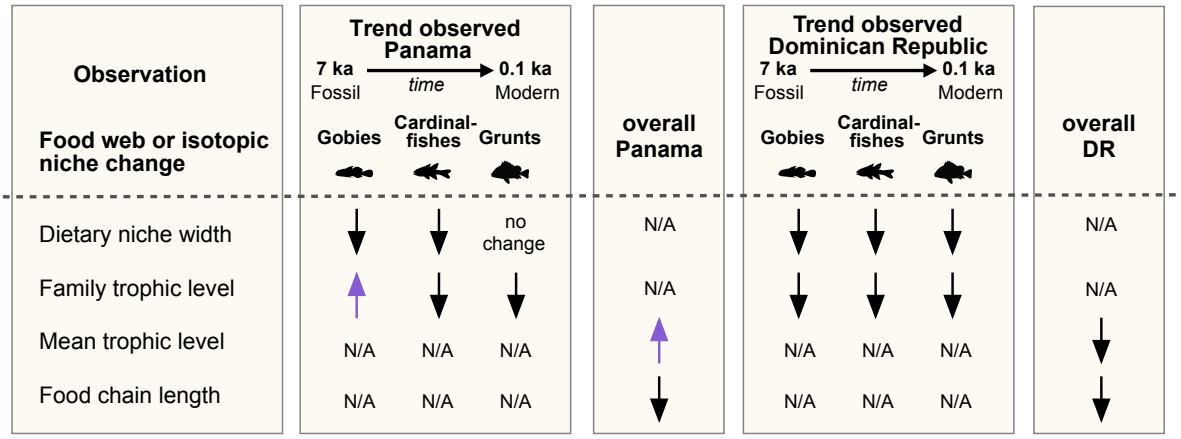

Fig. S7 | Summary figure showing all observations following bootstrapping results.

Table S1 | Range of otolith masses, reconstructed fish lengths, and N content for individuals from each of the four fish families. N content is also shown for coral. The total number of individuals (for fish) and fragments (for coral) measured in the current study are shown.

Family	Otolith mass (mg)	Reconstructed length (mm)	$\delta^{15}N$ ‰ range	$\delta^{15}N$ ‰ mean ± 1 SD	N content (nmols N mg^{-1} otolith) mean ± 1 SD	*n* individual fish or coral fragments
Goby	0.06-2.91	10-30	1.5-8.2	5.5 ± 1.7	39.5 ± 2.6	45
Cardinalfish	0.24-5.93	12-41	5.5-11	8.6 ± 1.8	36.4 ± 5.3	40
Silverside	0.53-5.71	13-33	7.4-9.4	8.2 ± 0.5	37.9 ± 5.1	19
Grunt	0.18-37.83	10-110	4.4-10.8	8.5 ± 1.2	42.5 ± 10.0	32
Coral	NA	NA	3.6-6.5	4.8 ± 0.6	4.1 ± 0.5	35

Table S2 | The unweighted MTL compared with the two MTL metrics referenced in the main text (the abundance-weighted MTL the measured MTL). The unweighted MTL is the unprocessed mean of all $\delta^{15}N$ measurements from each time period (see *Extended Data Fig. 4*).

	Fossil $\delta^{15}N$ ± 1 SD (‰)	Modern $\delta^{15}N$ ± 1 SD (‰)	$\delta^{15}N$ Change (‰)	Wilcoxon adjusted *P*-value, statistic (*W*), effect size (*r*)	Modern $\delta^{15}N$ (baseline corrected)	$\delta^{15}N$ change (‰) *vs.* fossil (baseline corrected)
Panama						
Unweighted MTL	7.74 ± 2.05[a]	7.90 ± 1.22[a]	0.16	P=0.99, W=1080, r=0.0016	8.39	0.65
Abund.-weighted MTL[b] (bootstrapped)	5.84 ± 1.3	7.15 ± 0.79	**1.32*****	**P=2.2x10^{-16}**, W=567, r=0.669	7.64	1.80
Measured MTL	8.02 ± 0.6[a]	8.07 ± 0.30 [a]	0.05	P=1.0, W=8, r=0	8.56	0.54
Dominican Republic						
Unweighted MTL	8.12 ± 2.7[a]	5.47 ± 1.50[1]	**-2.65*****	**P=1.5x10^{-4}**, W=387, r=0.580	5.86	-2.26
Abund.-weighted MTL[b] (bootstrapped)	6.05 ± 1.97	5.24 ± 0.82	**-0.81*****	**P=8.4x10^{-5}**, W=33018, r=0.176	5.63	-0.42
Measured MTL	7.90 ± 1.07	5.72 ± 0.53[1]	-2.18	P=0.4, W=7, r=0.445	6.11	-1.79

[a] Standard deviation estimates for FCL and MTL were calculated using error propagation. For all other categories, the variation (1 SD; niche width) of individuals within each family is reported.
[b] The abundance-weighted MTL was calculated by resampling the $\delta^{15}N_{oto}$ measurements for each family using bootstrapping and applying a resampled $\delta^{15}N_{oto}$ value to each otolith for each family in the sedimentary record, weighted by the number of otoliths. Thus, the abundance-weighted MTL reflects the relative abundances of each family in the sedimentary record (Methods).

Table S3 | Geographic locations of each locality.

	Mid-Holocene (fossil) Geographical Locations		
Region	**Stations**	**Longitude**	**Latitude**
Panama	Sunset Point	-82.270	9.360
	Sweet Bocas	-82.271	9.361
Dominican Republic	Cañon los Rios	-71.62	18.53
	Las Clavellinas	-71.55	18.50
	Sub-Recent (modern) Geographical Locations		
Panama	Playa Estrella	-82.33	9.40
	Punta Caracol	-82.30	9.38
	Casa Blanca New	-82.279	9.3619
	Casa Blanca	-82.284	9.3624
	STRI Point	-82.26	9.35
	Airport Point	-82.26	9.34
	SW Bocas Island	-82.25	9.33
	Cayo Adriana	-82.28	9.36
Dominican Republic	La Caleta Beach Reef	-69.69	18.45
	Hickory Ship, La Caleta	-69.68	18.43
	Wreck Limon La Caleta	-69.68	18.42

Table S4 | Highest resolution taxonomic classification of otoliths analyzed for $\delta^{15}N$.

	Family level	Genus level	Species level
Goby	33.3%	26.7%	40.0%
Silverside	NA	NA	100.0%
Cardinalfish	60.0%	40.0%	
Grunt	8.1%	62.2%	29.7%
Total	29.8%	36.2%	34.0%

Table S5 | Summary of data used to impute bootstrapped $\delta^{15}N$ community metrics. Measured $\delta^{15}N$ for each family and fish community composition are shown**.** The reef sedimentary deposits, which are time-averaged, capture the predator-excreted deposition of otoliths onto the reef sediments through time. The relatively high abundances of gobies (Gobiidae) and cardinalfishes (Apogonidae) reflect the high turnover rates (i.e., the short generation times and high mortality rates) of these groups.

Specimen type			Measurements				Bootstrap results	Fish community		
Region	Time period	Family	Mean (‰)	Median (‰)	1 SD (‰)	*n*	Mean (‰)	*n*	subtotals	proportion
Panama	Fossil	Goby	5.43	5.73	1.59	8	5.44	508		0.91
		Cardinalfish	9.94	9.91	0.96	7	9.93	49		0.09
		Grunt	8.80	8.78	0.97	8	8.81	2	559	0.004
	Modern	Goby	6.81	6.89	0.54	9	6.80	935		0.84
		Cardinalfish	8.98	8.70	0.83	3	8.99	169		0.15
		Grunt	8.55	8.58	0.51	13	8.55	13	1117	0.01
Dominican Republic	Fossil	Goby	5.26	6.10	2.85	5	5.26	126		0.95
		Cardinalfish	9.16	9.24	1.11	4	9.15	27		0.20
		Grunt	9.41	9.44	0.66	5	9.41	6	132	0.05
	Modern	Goby	4.46	3.90	1.92	6	4.46	174		0.51
		Cardinalfish	6.01	6.01	0.69	2	6.01	161		0.47
		Grunt	7.09	6.93	0.40	3	7.09	7	342	0.02